

International Conference on Space Optics—ICSO 2008

Toulouse, France

14–17 October 2008

Edited by Josiane Costeraste, Errico Armandillo, and Nikos Karafolas



Hydra multiple head star sensor and its in-flight self-calibration of optical heads alignment

L. Majewski

L. Blarre

N. Perrimon

Y. Kocher

et al.



HYDRA MULTIPLE HEAD STAR SENSOR AND ITS IN-FLIGHT SELF-CALIBRATION OF OPTICAL HEADS ALIGNMENT

L. Majewski ⁽¹⁾, L. Blarre ⁽¹⁾, N. Perrimon ⁽¹⁾, Y. Kocher ⁽¹⁾, P.E. Martinez ⁽²⁾, S. Dussy ⁽³⁾

⁽¹⁾ EADS-SODERN, 20 avenue Descartes, 94451 Limeil Brévrannes Cedex, France,
laurent.majewski@sodern.fr, ludovic.blarre@sodern.fr, nicolas.perrimon@sodern.fr, yves.kocher@sodern.fr

⁽²⁾ CNES, 18 Avenue Edouard Belin, 31401 Toulouse Cedex 9, France
pierre-emmanuel.martinez@cnes.fr

⁽³⁾ ESA-ESTEC, Keplerlaan 1, 2201 AZ Noordwijk, The Netherlands
Stephane.Dussy@esa.int

ABSTRACT

HYDRA is EADS SODERN new product line of APS-based autonomous star trackers. The baseline is a multiple head sensor made of three separated optical heads and one electronic unit. Actually the concept which was chosen offers more than three single-head star trackers working independently. Since HYDRA merges all fields of view the result is a more accurate, more robust and completely autonomous multiple-head sensor, releasing the AOCS from the need to manage the outputs of independent single-head star trackers.

Specific to the multiple head architecture and the underlying data fusion, is the calibration of the relative alignments between the sensor optical heads. The performance of the sensor is related to its estimation of such alignments.

HYDRA design is first reminded in this paper along with simplification it can bring at system level (AOCS). Then self-calibration of optical heads alignment is highlighted through descriptions and simulation results, thus demonstrating the performances of a key part of HYDRA multiple-head concept.

1 INTRODUCTION

The appearance of a new generation of APS detectors specially designed for Star Sensors use was the opportunity for SODERN to develop a new product line of star trackers. The properties of the new APS detectors allow in themselves significant mass, power and cost benefits, but also permitted to propose a new Star Sensor concept.

CMOS technology made it easier to separate the sensing element, the Optical Head, from the power supply and processing units. This gave access to a new multiple head architecture with challenging data fusion and autonomous management of optical heads alignments for major breakthrough in performances, robustness and autonomy.

2 HYDRA DESCRIPTION

2.1 Architecture

The design is based on two physically independent units, the Optical Head (OH) and the Electronic Unit (EU). Each OH performs the star detection including low level signal processing inside a FPGA or ASIC in order to reduce the amount of EU data processing. The useful processed video signal is then transferred to the EU, at high data rate (thanks to the SpaceWire data interface between optical heads and EU). Higher level computation like star pattern identification, star tracking and attitude data computation are performed by the embedded software in the electronic unit, with true attitude update rates up to 30 Hz on three heads.

The baseline of the HYDRA concept is an assembly of three optical heads processed by a single centralized electronic unit. This architecture provides an extremely reliable configuration. The hardware architecture can nevertheless be adapted to the mission requirements with either a hot or cold redundancy scheme for the heads (up to four heads with one in cold redundancy) and a single or a two electronic unit scheme for cold redundancy (see Fig. 1 and [1]).

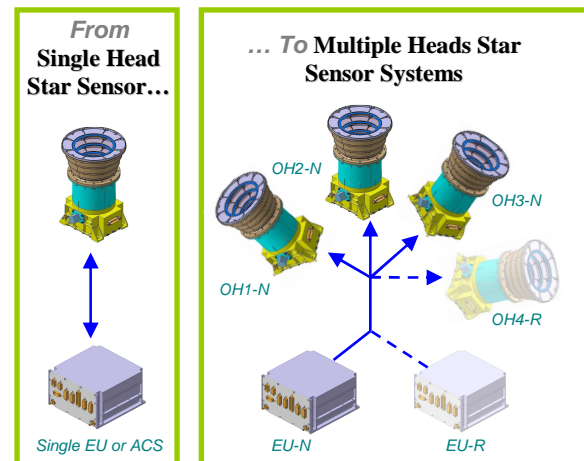


Fig. 1. Various HYDRA possible configurations.

2.2 Optical Head design

The Optical Head (OH) has been designed with performance, flexibility, cost, mass and power efficiency in mind. Its low mass and stiff compact design authorize the unit to survive very severe mechanical environmental conditions enabling compatibility with a very wide range of launchers and easy placement anywhere on a s/c while requiring no special mounting brackets.

The OH is constituted of the following main elements:

- A detection module, made of an HAS APS detector from Cypress and a thermo-electric cooler,
- A radiation hardened optic with a wide circular field of view of 22°,
- The electronic for the internal secondary power supplies regulation and distribution,
- The electronic logic for detector and video pre-processing, with a FPGA for customized processing or an ASIC for the generic processing,
- A baffle made of aluminium to trap straylight,
- A baffle support structure made of titanium for a good thermal insulation of the baffle,
- An aluminium housing to ensure mechanical and thermal stability.

The detector temperature is maintained at a +15°C temperature by the Peltier cooler such that the detector can operate with nominal performances in a wide range of base plate temperatures (-30°C to +60°C - qualification range). This detector operating temperature allows also a very low power dissipation of about 1 Watt for an average base plate temperature around +20°C with hence an excellent thermal stability and an easy implementation on the optical bench for high accuracy applications.

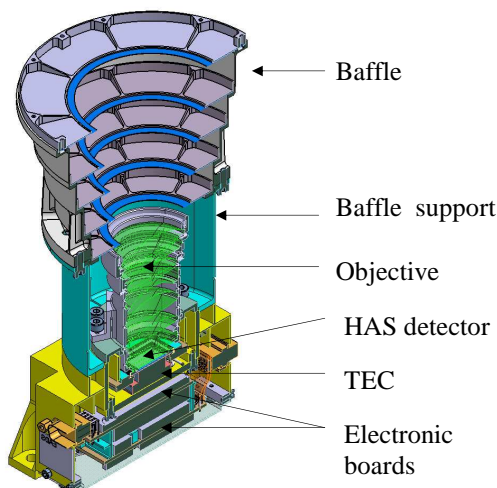


Fig. 2. Cut away view of HYDRA Optical Head.

2.3 Electronic Unit design

The Electronic Unit (EU) is a monolithic box that contains both the Processing Unit and the Power Supply. The EU thus presents a single point interface between the Star Sensor System and the AOCS, and centralizes all the data emitted by the OH preventing the need to connect the AOCS to each head separately.

The Electronic Unit main purposes are, on one hand, to compute from each OH data the attitude quaternion and angular rate, and on the other hand to generate and distribute all the power supplies needed by the Star Sensor Optical Heads. It can be easily adapted to various configurations:

- Drive one up to three heads plus one more connected in cold redundancy,
- Redounded with two electronics able to address the same heads,
- Can be installed up to 15 meters away from the heads.

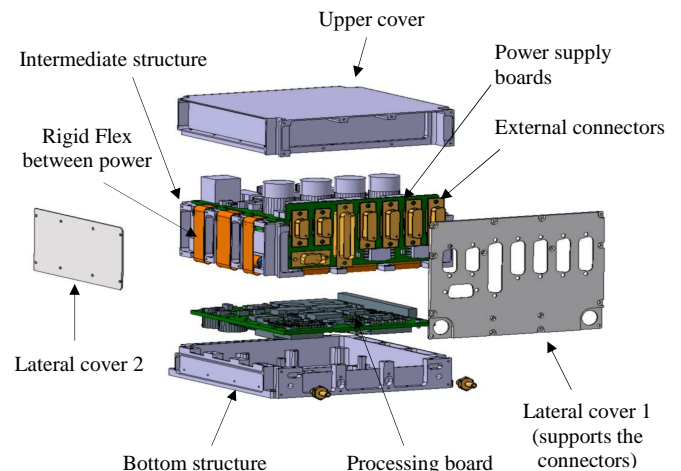


Fig. 3. HYDRA Electronic Unit exploded view.

2.4 Software design and Operating Modes

The software is organized in two main parts (Fig. 4):

- The basic software directly deals with hardware and is in charge of data interfaces and non mission modes: stand-by, self test, memory reading and writing.
- The application software is in charge of the mission modes: Angular Rate Mode for autonomous rate determination, Attitude Acquisition Mode for autonomous "lost in space" attitude determination and Attitude Tracking Mode for recurrent autonomous attitude determination with a priori knowledge of attitude.

This architecture allows an easy adaptation of the HYDRA software to different types of applications by changing only the application software developed with automatic coding tools from The MathWorks™ (Simulink and Real-Time Workshop Embedded Coder).

In Angular Rate and Acquisition modes, each head is processed identically but independently one after the other to share the processor load equally between the heads. The acquisition is based on full frame images with double integration to remove the charged particles induced transient effects (protons, electrons, heavy ions,...). The rate is first estimated by a relative attitude determination between objects detected on images of two following cycles. Then the image can be corrected from rate image distortion arising from the HAS rolling shutter mode and the star pattern recognition algorithm is used to match the measured stars with the stars of the catalogue and determine a first attitude.

Once full acquisition process is done on one head, the application software switch to Autonomous Tracking Mode, which is a more performing and robust operating mode using a priori knowledge of the attitude to designate the stars to be measured by the optical heads on small measurement windows. In this mode the heads are all operated synchronously at a rate of up to 30 Hz with tracking of up to 15 stars per heads used to refresh both single head and fused multiple head attitude data.

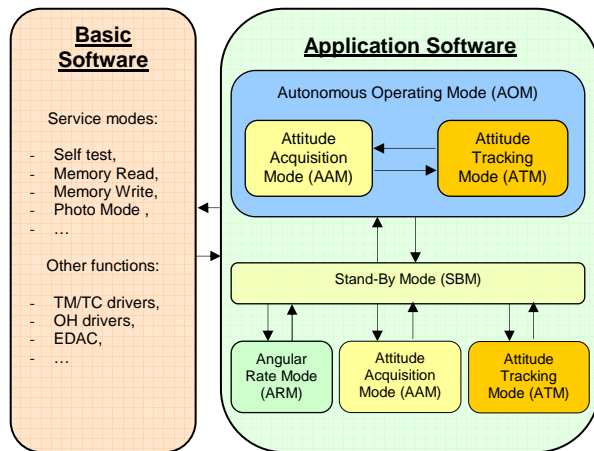


Fig. 4. HYDRA software and operating modes.

2.5 Main Budgets and Performances

HYDRA generic design was made on purpose to meet a wide variety of missions, including all types of orbits (LEO, MEO, GEO, deep space) as well as various types of platforms (from small and very agile one to

big and low rate one). This induced some minimum available configurations for data interface format, data rate, type of power supply. It also included a qualification for rather severe and enveloping environmental conditions. All of this is summarized in Table 1.

Table 1. HYDRA main features.

Mass of sub-assemblies
<ul style="list-style-type: none"> OH with: <ul style="list-style-type: none"> 40° SEA / 30° EEA baffle: 1.3 kg 30° SEA / 29° EEA baffle: 1.45 kg 25° SEA baffle: < 1.7 kg One Electronic Unit for three OH's: 1.7 kg
Sub-assemblies Dimensions
<ul style="list-style-type: none"> OH : H=139 mm x L=90 mm x l=111 mm 40°-baffle : H=85 mm x Φ=131 mm 30°-baffle : H=147 mm x Φ=145 mm 25°-baffle : H=188 mm x Φ=162 mm (TBC) EU : L=145 mm x l=158 mm and H=99 mm
Power consumption
<ul style="list-style-type: none"> 1 W per OH @20°C interface (IF) temperature 11.2 W total for 3 OH's and 1 EU operating @20°C IF 14.7 W total for 3 OH's and 1 EU operating @40°C IF
Maximum base plate temperature
<ul style="list-style-type: none"> -30°C to +60°C for OH and -30°C / +65°C for EU
Mechanical environment
<ul style="list-style-type: none"> Random 29 grms Shock level: 1500g SRS
Parts
<ul style="list-style-type: none"> ITAR free with ASIC or ITAR with FPGA Space level 1(QMLV) or Space level 2 (QMLQ)
Attitude output frequency
<ul style="list-style-type: none"> Up to 30 Hz - real three heads output data
Robustness
<ul style="list-style-type: none"> High proton flux in all modes (SAA, solar flares) Keep Tracking with only one available OH (Sun and Earth crossing) Nominal operation with Moon in the FOV Angular rates up to 10°/s, acceleration up to 10°/s²
Reliability
<ul style="list-style-type: none"> 200 / 250 fits for each OH for EEE parts level 1/2 700 / 900 fits for one EU for EEE parts level 1/2
Lifetime
<ul style="list-style-type: none"> LEO 7 years or GEO 18 years
Interface type with AOCS
<ul style="list-style-type: none"> MIL 1553B or RS422 (AS16/CS16)
Input power need
<ul style="list-style-type: none"> 20V-55V or 50V-105 V power bus
Modular design options
<ul style="list-style-type: none"> Fourth OH in cold redundancy Gyros input or low cost gyro Various configurations possible with only 1 or 2 OH's Centralized processing in On Board Computer

Fused multiple head concept of HYDRA extends star tracker field of view providing robustness to occultation of one or two OH's from external bodies

like Sun and Earth with then attitude update provided by only one or two available optical heads.

From accuracy point of view single head architecture leads to more noisy measurements around boresight axis compared to cross boresight axes, while a three OH's orthogonal configuration gives better and true equalized 3-axis performances.

Tables 2-5 give an overview of HYDRA measurement accuracy for the baseline configuration with three operating optical heads, but also with only one or two heads available to account for degraded performances in case of blinding on one or two heads. The accuracy figures encompass typical "worst case" EOL conditions of 7 year LEO or 18 year GEO missions. Other hypotheses that were made for the assessment are reminded hereafter:

- Optical heads with orthogonal orientation,
- No thermo-elastic distortions between OH's from satellite structure (rigid structure),
- 40° baffle with Sun at 40° from one head and Earth limb at 30° from a second head,
- Accurate stabilization of OH's mounting planes temperatures (20±3° C) and large temperature fluctuations ([-20..+50] ° C),
- Angular rates ranging from 0.2°/s to 5°/s,
- HAS detector maintained at +15°C,
- 30Hz output rate,
- Performance statistics assessed from 200000 randomly drawn attitudes over the celestial vault.

Whatever the considered axis is, the systematic attitude measurement error is below 10 arc seconds.

Table 2. Bias maximum error in arcsec.

Bias (", max)	1 OH	2 OH's	3 OH's
X/Y		7.5	
Z		10	

Low Frequency Errors (LFE) in attitude measurement arise from both thermo-elastic behaviour of OH's (thermal LFE) and also non uniformities in fields of view properties (FOV error).

Thermal LFE account for drifts of OH's lines of sight as a function of base plates temperature variations.

Table 3. Thermal LFE at 3σ in arcsec.

Thermal LFE (", 3σ)	1 OH	2 OH's	3 OH's
20±3° C	X	0.4	0.2
	Y		0.3
	Z	0.0	0.2
[-20..+50] ° C	X	4.1	1.8
	Y		3.5
	Z	0.0	1.8

FOV error depends both on change of star patterns location within FOV and imaging thermal conditions.

Table 4. FOV error at 3σ in arcsec.

FOV error (", 3σ)	1 OH	2 OH's	3 OH's
20±3° C	X	1.4	1.4
	Y		1.0
	Z	6.6	1.4
[-20..+50] ° C	X	1.7	1.6
	Y		1.2
	Z	8.5	1.6

LFE error is lower than 1.5 arcsec (3σ) with the accurately regulated mounting plane temperature. In this case the thermal LFE is almost negligible compared to FOV error. Moreover studies are currently carried out to yet improve FOV error budget. For large temperature fluctuations, the two contributions are of similar amplitude.

Noise Equivalent Angle (NEA) is the high frequency error that is made up of temporal noise, pixels non uniformities and pixel discretization of the detector. It changes first with angular rate. Low angular rates only require splitting between temporal noise and pixel-to-pixel error. At higher rates temporal and pixel spatial noises merge.

Table 5. NEA at 3σ in arcsec (30Hz).

NEA (", 3σ)	1 OH	2 OH's	3 OH's	
0.2°/s	temporal noise	X	8.2	8.0
		Y		5.4
		Z	66	8.0
	pixel-to-pixel noise	X	3.4	3.3
		Y		2.3
		Z	27	3.3
1°/s	X	9.5	8.7	
	Y		6.0	
	Z	75	8.7	
5°/s	X	20	14	
	Y		9.3	
	Z	160	14	

3 SELF-CALIBRATION OF OPTICAL HEADS ALIGNMENT

As soon as it was imagined, HYDRA was intended to provide more than several star trackers working independently. The design driver for multiple-head configuration was to profit from several optical heads that would share data to bring more accuracy and more robustness to the overall star sensor system. A fusion concept emerged where the accurate knowledge of the alignment between optical heads quickly proved to play an important role to greater improve the efficiency of the data fusion. Indeed the autonomy of the sensor

had to be preserved so the in-flight estimation of the alignment between heads had to be done by the sensor itself.

3.1 Fusion concept

HYDRA fusion basically consists of converting star unit vectors from all optical heads to a common reference frame and then to compute a consolidated 3-axis attitude from these vectors. One optical head is chosen to provide such frame, so the fusion process obviously requires the rotation transformations between heads. These transformations are usually calibrated on ground but with accuracies of tens of arc seconds that prevent to reach the best fusion performance. Moreover mechanical shifts of optical heads may occur during spacecraft launch increasing again the misalignments. HYDRA copes with it by using the single optical head attitudes to update these calibrations in-flight at the very beginning of the use of the unit. This self-calibration process not only allows correcting the initial lack of knowledge of OH's alignment but also tracks the current distortions between heads that may arise from in-flight thermo-elastic distortions of the spacecraft structure.

Thanks to its self-calibration capability HYDRA should require for most missions that only one optical head be as stable as possible to some spacecraft reference (for instance the optical bench of a payload). HYDRA will compute an optimised attitude of this user defined external reference head by merging all optical heads star data, and will deliver it in its telemetries in addition to usual single head quaternions that are computed for each optical head seen as single star trackers.

The fusion concept should thus have positive impacts on design, integration and operation of star sensor on-board spacecrafts. While keeping one optical head very stable, spacecraft system designers could consider releasing some mechanical stability requirements of the other heads on-board platforms since the star sensor will deal with relative angles. This should not only simplify the system design but also make the integration of multiple heads easier, thus saving time and cost. Indeed the existence of a stable frame within the star sensor elements attractively limits jumps of attitude measurements over time. To some extent, only the alignment of the external reference head with the spacecraft reference could be considered to be calibrated in flight, simplifying also the in-flight management of the sensor at system level (AOCS).

3.2 Fusion performance versus alignment estimation error: a theoretical insight.

The errors of rotation transformations between optical heads are easily analysed in the case of an orthogonal installation of the heads as depicted in Fig. 5, where Z_i vectors are the lines of sight, and the different reference frames axes are parallel.

Let R_{OH1} and R_{OH2} be the measurement reference frames of optical heads number 1 and 2. R_{OH1} is chosen as the common frame for the fusion of star data. Q_{21} is the transformation quaternion enabling to bring R_{OH2} into coincidence with R_{OH1} . This quaternion is computed from quaternions Q_1 and Q_2 which render OH's attitudes relatively to the celestial vault's inertial frame with standard deviation σ_{XY} (respectively σ_z) around cross-boresight axes (respectively boresight axis) of each single head frame.

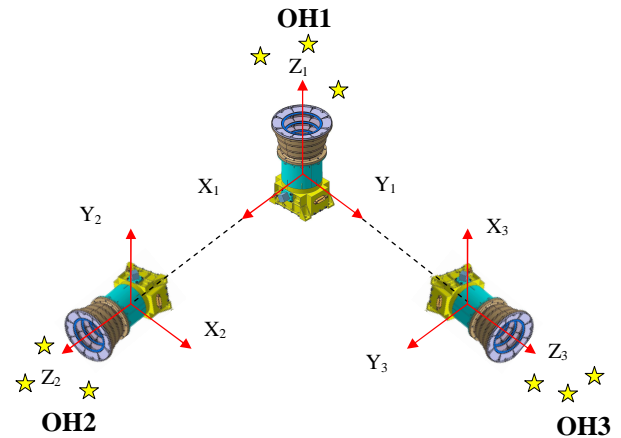


Fig. 5. Orthogonal installation of OH's.

Q_1 and Q_2 single head measurements are independent, so their error variances combine linearly causing Q_{21} to have following error variances about R_{OH1} axes:

$$\begin{cases} \sigma_{21/X1}^2 = \sigma_{xy}^2 + \sigma_z^2 \\ \sigma_{21/Y1}^2 = 2\sigma_{xy}^2 \\ \sigma_{21/Z1}^2 = \sigma_{xy}^2 + \sigma_z^2 \end{cases} \quad (1)$$

Eq. 1 clearly shows that single head measurement error around boresight axis, which is several times higher than cross-boresight errors, impacts the accuracy of Q_{21} about two axes of the fusion frame R_{OH1} . Same form of relation is found for the transformation quaternion from OH_3 to OH_1 , with a permutation in R_{OH1} axes. Since fusion of star data will make use of transformation quaternions, low pass filtering of Q_{21} is considered to

reduce noise, resulting in attenuation factors α that apply to variances of Eq. 1.

From error variance analysis point view, the fusion process leading to the determination of OH₁ attitude using star measurements from all optical heads can be analysed as the combination of three independent attitude measurements of OH₁ reference frame (one per OH) where transformation quaternions are used to infer additional OH₁ attitude measurements from the other heads.

Two hypotheses are then made to carry on theoretical analysis and assess fusion performance. First, time filtering of transformation quaternions allows considering that residual errors are highly decorrelated from noise of instantaneous single head quaternions. The error variance of OH₁ attitude computed for instance from OH₂ measurements is thus the sum of OH₂ error variance and Q₂₁ error variance. Second, the appropriate weighting of stars allows considering that the combination of measurements tends to be statistically optimal.

Fig. 6 shows the results of such variance analysis in the form of the ratio of noise (in short for error standard deviation) between fused multiple-head and single-head measurements as a function of the transformation quaternions filtering factor α .

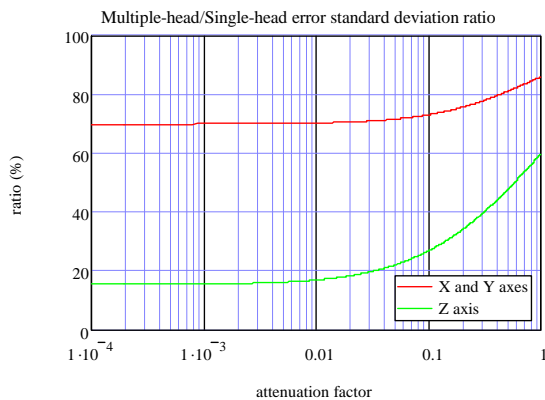


Fig. 6. Multiple head/single head noise ratio.

α equals 0 means that transformation quaternions are perfectly filtered. In this case the fusion is optimal and multiple-head noise is about 70% of single-head noise about X and Y axes, and only 15% of single-head noise about Z axis. Multiple head sensing reduces errors around boresight axis to the level of those around cross-boresight axes.

Conversely, α equals 1 when transformation quaternions are either not filtered or when the filter is not efficient for the errors that are considered. The fusion is then sub-optimal, though fused multiple-head

noise is only 85% of single head noise about X and Y axes, and 60% of single-head noise about Z axis.

The analysis shows that whatever the filtering performances are, the multiple head performance overtakes the accuracy achieved with only one head.

Another useful curve for multiple head performance assessment is the deviation relatively to fusion optimal performance as a function of filtering factor α . Fig. 7 illustrates the relative degradation of optimal fusion noise (in short for error standard deviation) when α ranges from perfect filtering ($\alpha = 0$) to inefficient filtering ($\alpha = 1$).

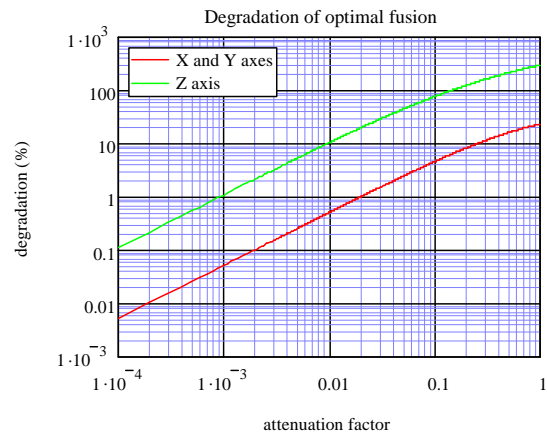


Fig. 7. Deviation from optimal fusion.

Sub-optimal fusion does not deviate more than about 10% from optimal fusion provided that filtering performances allow to lower transformation quaternions noise by a factor of 100 or better.

3.3 Kalman-based estimation of optical heads alignment: simulation results.

HYDRA optical heads alignment estimator is a discrete Kalman filter based on a time-invariant distortion state model. It is built on the classical two stage scheme: current alignments of optical heads are predicted first using the state models and then are corrected based on measured alignments inferred from single head attitudes.

The performance of the estimator has been investigated for three classes of missions:

- High performance mission corresponds to a high stability mounting plane temperature ($\pm 1^\circ\text{C}$ over one orbit in LEO) and rigid satellite structure supporting OH's base plates. For this class of mission, convergence time is defined as the time needed to reach 99% of the FOV performance (error increase limited to 1 %).

- Medium performance mission corresponds to a rigid satellite structure supporting OH's base plates, and larger mounting plane temperature fluctuation ($\pm 15^\circ\text{C}$ over one orbit in LEO). For this class of mission, convergence time is defined as the time needed to reach 80% of the FOV performance (error increase limited to 20%).
- Low performance mission corresponds to a satellite structure with fast and significant deformations (± 2 arc minutes over one orbit in LEO) that need to be tracked by the filter. For this class of mission, the convergence time is defined as the time needed to limit FOV error increase to 100 %.

The simulations suppose that the heads are installed orthogonally and rotate at $1^\circ/\text{s}$ in EOL conditions of a LEO mission. The sensor errors have been modelled carefully in the frequency domain to render single head NEA, thermal LFE and FOV error to account for filter performances with coloured measurement errors.

The Kalman filter is tuned in order to either achieve noiseless estimation of transformation quaternions between heads (with then no track of inter-head distortions), or fast track OH's relative motions (with then noisiest estimation). The former suits well to high performance mission with high thermal and mechanical stabilities (see Fig. 8), while the latter is rather intended for lower performance missions where non negligible thermo-mechanical instabilities occur (see Fig. 9).

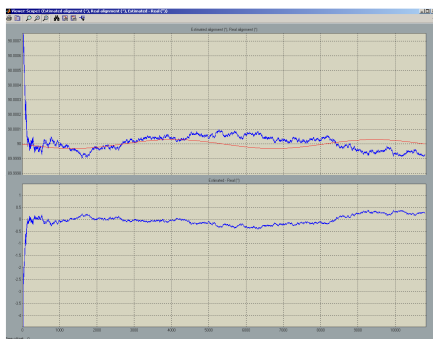


Fig. 8. Self-calibration - high performance mission.

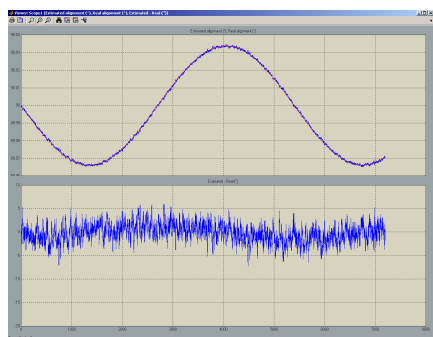


Fig. 9. Self-calibration - low performance mission.

The error variance of the estimation process has been computed from residual errors of alignments estimates over time. This value, along with error variance of raw measurements of alignments, enables to determine the attenuation coefficients α mentioned earlier and summarized in Table 6.

Table 6. Filtering performances.

Mission performance class	Error class	Filtering performance	
		Attenuation factor	Convergence time
High	NEA	1.67×10^{-5}	~300 s
	FOV error	1.37×10^{-3}	
Medium	NEA	2.28×10^{-4}	~60 s
	FOV error	1.80×10^{-2}	
Low	NEA	1.67×10^{-3}	~10 s
	FOV error	0.176	

From then on Fig. 7 provides the expected degradation of both NEA and FOV error with respect to optimal fusion for the different missions (see Table 7).

Table 7. Self-calibration impacts on performances.

Mission performance class	High	Medium	Low
Conditions	$20 \pm 3^\circ\text{C}$ No thermo-elastic distortion from satellite	$20 \pm 15^\circ\text{C}$ No thermo-elastic distortion from satellite	$20 \pm 15^\circ\text{C}$ Thermo-elastic distortion from satellite = ± 2 arc minutes
Convergence time at $1^\circ/\text{s}$	~300 s	~60 s	~10 s
NEA degradation	< 0.1%	< 1%	< 10%
FOV error degradation	~1.5%	~20%	$\times 2$

4 CONCLUSION

A complete campaign of tests, ranging from performance characterization to mechanical and thermal environment tests at qualification level, has been successfully performed on the Optical Head Engineering Model. It has allowed characterizing finely the Sensor elementary performances. These results have been used to feed a detailed and accurate modelling of the sensor in order to consolidate the performance budget taking into account innovative data fusion and self-calibration of OH's alignments. These performances fulfil HYDRA specifications and, along with other multiple head features, will pave the way for a breakthrough in satellite attitude control.

5 REFERENCES

1. Blarre L., et al. "Innovative G&C solutions enabled by new generation of sensors" AAS 08-007